

# From Actively Impedance Controlled Light-weight Robot Hands to Intrinsically Compliant Systems

T. Wimböck, M. Grebenstein, M. Chalon, W. Friedl, Ch. Ott, A. Albu-Schäffer, and Gerd Hirzinger

Institute of Robotics and Mechatronics  
German Aerospace Center (DLR)

**Abstract**—The consideration of uncertainties in robotic manipulation tasks is often significant to achieve a reliable and successful operation. This becomes especially relevant in the case of unstructured environments. This paper focuses on considering uncertainties from a design and control perspective. It is well known that impedance control can be used to account for position uncertainties. The compliance properties that are given to the controlled system avoid that excessively large forces are exerted on the environment. We present several applications for robotic hands and furthermore an impedance controller for torque controlled complex kinematic chains. However, the mechanical robustness for such, rather stiff, systems is limited and much lower than that of humans. Further, the reaction time of the actively controlled compliance is bounded. Embedding the compliant behavior directly in the robotic design is therefore a solution that gives two benefits. On the one hand the compliant features help to cope with position uncertainty, and on the other hand the introduced mechanical compliance acts as mechanical low pass filter to external forces, and therefore protects the gears and motors. The hand subsystem of the DLR hand arm system is presented here, that possesses significantly increased robustness and flexibility at the same time.

## I. INTRODUCTION

In robotic manipulation tasks, uncertainty plays a crucial role. This becomes especially relevant in the case of unstructured environments. The robustness of task execution can be improved by special measures in several fields, in particular the manipulator design, the control strategy, and the higher-level planning methods. This paper focuses on the first two topics. It is well known that impedance control can be used to account for position uncertainties. The compliance properties that are imposed to the controlled system avoid that excessively large forces are exerted assuming that the controller parameters are chosen appropriately. In the case of grasping actions this leads to a robust behavior w.r.t. geometrical object properties and contact point uncertainties. Furthermore, in this case no contact detection nor controller switching is needed compared to hybrid force position controlled approaches. With this concept interesting applications can be developed. However, the mechanical robustness as well as the reaction time of the actively controlled compliance are limited. Embedding the compliant behavior directly in the robotic design is therefore a solution that gives two benefits. On the one hand the compliant features help to cope with position uncertainty and on the other hand the introduced mechanical compliance acts as mechanical low pass filter to external forces and therefore protects the gears



Fig. 1. DLR's humanoid Robot Justin.

and motors. This way, the robustness of the robotic system is increased significantly.

We will start by reviewing the main control ideas of actively controlled compliant systems using as examples the DLR arms, hands, and the humanoid manipulator Justin (Fig. 1). We are taking these robots as a performance reference, which we are currently trying to outperform with new variable stiffness actuators. This will lead us to the motivation of the design of a robot hand with variable stiffness (Fig. 2). We will present the main design ideas and our first results with the new prototype. An experiment using a hammer provides first validation of the gain of this novel concept.

Note that this overview paper is based on the article [1] for the first part, and the second part is taken from [2]. Please

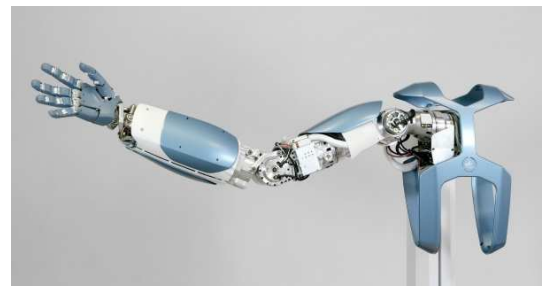


Fig. 2. DLR hand arm system.

find the discussion of the state of the art therein.

## II. COMPLIANCE CONTROL FOR LIGHT-WEIGHT ROBOTS

In the next two sections, the framework used to implement active compliance control based on joint torque sensing is summarized. The light-weight design is obtained by using relatively high gear reduction ratios (typically 1:100 or 1:160), leading to joints which are hardly backdrivable and have already moderate intrinsic compliance. Therefore, we model the robot as a flexible joint system. Thus, measuring the torque after the gears is essential for implementing high performance soft robotics features. When implementing compliant control laws, the torque signal is used for reducing the effects of joint friction, and in the case of the arms as well as to damp vibrations related to the joint compliance. Motor position feedback is used to impose the desired compliant behavior. The control framework is constructed from a passivity control perspective, by giving a simple and intuitive physical interpretation in terms of energy shaping to the feedback of the different state vector components.

In order to simplify the analysis and to be able to generalize the joint level approach also to Cartesian coordinates, the idea of interpreting the joint torque feedback as the shaping of the motor inertia plays a central role [3], [4].

Using motor position  $\theta$  for control and not the link position  $q$  is essential for the passivity properties of the controller. However, the desired position and stiffness are usually formulated in terms of the link position. For the impedance controllers of the DLR light-weight robots, the position feedback has the form

$$u = -\frac{\partial V_P(\bar{q}(\theta))}{\partial \theta} - D_\theta \dot{\theta} + g(\bar{q}(\theta)) \quad (1)$$

with  $u$  being the input to the torque controller,  $V_P$  a positive definite potential function, and  $D_\theta$  a positive definite damping matrix chosen for a well damped transient behavior [5]. This is the classical structure of a compliance controller for rigid robots, except for the fact that, instead of the link position  $q$ , a position signal  $\bar{q}(\theta)$  is used, which is *statically equivalent* to  $q$ , i.e.  $\bar{q}(\theta) = q$  if  $\dot{q} = \dot{\theta} = 0$  and can be computed numerically<sup>1</sup> [3], [4].

Since now the position feedback is again only a function of  $\theta$ , the passivity of the controlled robot is given with respect to the input-output pair  $(\tau_{ext}, \dot{q})$ .

In order to obtain a joint level impedance controller, one can simply use  $V_P(\bar{q}) = \frac{1}{2}(\mathbf{q}_d - \bar{\mathbf{q}})^T K_J(\mathbf{q}_d - \bar{\mathbf{q}})$ , while for Cartesian impedance control  $V_P$  is defined as function of the Cartesian coordinates  $\mathbf{x}(\bar{\mathbf{q}})$  as detailed in section Sec. III. The external torque  $\tau_{ext}$  is then replaced by the external force<sup>2</sup>  $\mathbf{F}_{ext}$ . A Lyapunov function for the system is obtained by summing the kinetic and the gravity-potential energy of the rigid part of the robot dynamics with the kinetic energy of the scaled motor inertia and the potential energy of the controller [3], [4].

<sup>1</sup>In practice we often use indeed the trivial approximation  $\bar{q}(\theta) = \theta$  for applications in which high position accuracy is not required.

<sup>2</sup>The relation between the external tip force  $\mathbf{F}_{ext}$  and the external joint torque  $\tau_{ext}$  is  $\tau_{ext} = \mathbf{J}(\bar{\mathbf{q}})^T \mathbf{F}_{ext}$ .

## III. IMPEDANCE CONTROL FOR COMPLEX KINEMATIC CHAINS

We show how to apply the impedance control concept from the previous section to kinematically more complex robot systems, like artificial hands and anthropomorphic two-handed manipulator systems.

The design of appropriate potential functions  $V_P(\bar{\mathbf{q}})$  is the topic of this section. Furthermore, we will assume the potential function  $V_s$  of a virtual spatial spring, like e.g. the ones designed in [6], [7], [8], as a basic building block. This potential function  $V_s(\mathbf{H}_1, \mathbf{H}_2, \mathcal{K})$  depends on two frames  $\mathbf{H}_1 \in SE(3)$  and  $\mathbf{H}_2 \in SE(3)$  between which the spring is acting, and also on some configuration-independent internal parameters  $\mathcal{K}$ , like the stiffness values or the rest length.

### A. Artificial Hands

The DLR hand II is equipped with joint torque sensors in addition to joint position measurements. Therefore, it is possible to apply the impedance control aspects as presented in the previous section to our anthropomorphic robot hand. The feedback of the torque sensors is used to increase the backdrivability, respectively the sensitivity, of the joints. Due to the small link masses and the high mechanical joint stiffness, vibration damping is not an issue here. Therefore, the approximation  $\mathbf{q} = \boldsymbol{\theta} = \bar{\mathbf{q}}$  can be made.

The impedance control for hands can be used with different task coordinates. The hand will be often in contact with an object and therefore the concepts of impedance control can be fully exploited<sup>3</sup>. For power grasps joint level impedance control is applied. A pragmatic way to realize power grasps is to teach two joint configurations: One to preshape the hand and the second one with the virtual equilibrium position within the object, such that internal forces are applied. This way it is easy to e. g. grasp a spray can or to catch a ball (c.f. Fig. 3).

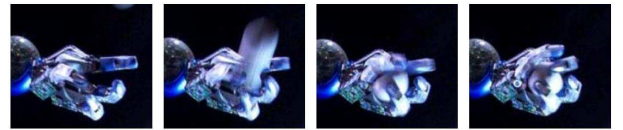


Fig. 3. Catching a flying ball using a power grasp realized by joint impedance control.

If the fingers have to be positioned separately from each other (e.g. the use of a touchpad or playing the piano (see Fig. 4)), it is useful to apply Cartesian fingertip control. The impedance control is used here to decrease the stiffness along the direction of contact whereas the stiffness for the lateral positioning over the keyboard is high. By modulation of the trajectories to press the keys, the playing volume was adjusted. In Fig. 5 the recorded piano sounds demonstrate the capabilities to generate many loudness levels between pianissimo and fortissimo.

<sup>3</sup>Beside grasping a hand has to be able to perform also tasks like gesticulation. However, in this case no particular positioning accuracy is required.

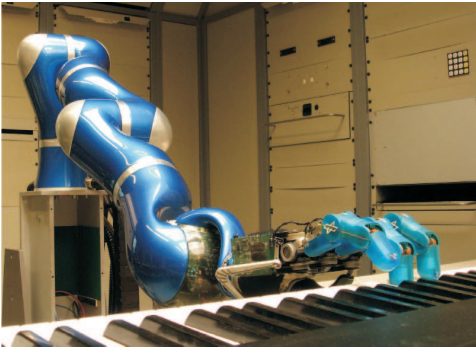


Fig. 4. DLR Hand II playing piano.

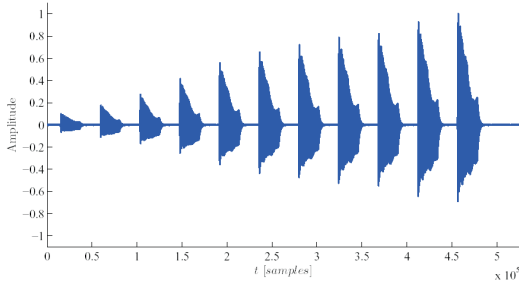


Fig. 5. Recorded piano sound signal demonstrating the ability to play at varying loudness.

The most interesting case from a control point of view is the fine manipulation of a grasped object since all degrees of freedom of the hand need to be coordinated to its motion. In this case the combined system containing arm, hand, and object represents a parallel robot (Fig. 6). The task coordinates consist of two contributions. On the one hand the Cartesian coordinates of the grasped object, on the other hand the coordinates that are related to internal forces. In [9] we introduced a passivity-based object-level controller for a multifingered hand based on a virtual object similar to [10]. In contrast to the IPC [10] the object frame is defined uniquely by the  $i = 1 \dots N$  Cartesian fingertip

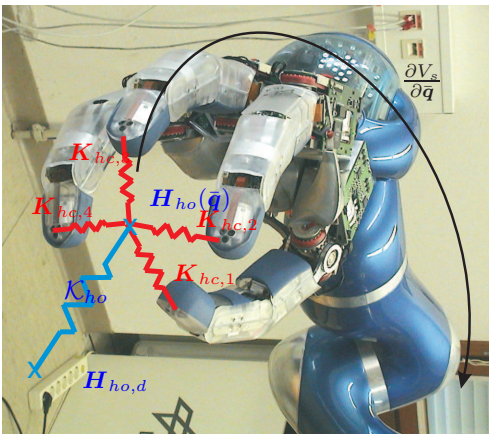


Fig. 6. DLR Hand II superimposed by the virtual springs defined by the potential functions in (2) and the virtual object.

positions  $\mathbf{p}_i(\bar{\mathbf{q}})$  by an appropriate kinematic relationship. The definition is such that it enables the spanning of the null-space of the grasp matrix by internal forces generated by virtual elastic elements connecting the virtual object frame with the finger tips (Fig. 6).

The definition of a potential function  $V(\bar{\mathbf{q}})$  to derive an object level controller is then described by the superposition of two potentials: the potential of a spatial spring  $V_s(\mathbf{H}_{ho}(\bar{\mathbf{q}}), \mathbf{H}_{ho,d}, \mathcal{K}_{ho})$  between the virtual object frame  $\mathbf{H}_{ho}(\bar{\mathbf{q}})$  and a virtual equilibrium frame  $\mathbf{H}_{ho,d}$  and a potential  $V_{hc}(\bar{\mathbf{q}}, \mathcal{K}_{hc})$  describing the  $i^{th}$  spring connecting the virtual object with the  $i^{th}$  frame of the fingertips  $\mathbf{H}_{f,i}(\bar{\mathbf{q}})$  for  $i = 1 \dots N$  that are used to generate internal forces, i. e.

$$V_P(\bar{\mathbf{q}}) = V_s(\mathbf{H}_{ho}(\bar{\mathbf{q}}), \mathbf{H}_{eq}, \mathcal{K}_{ho}) + V_{hc}(\bar{\mathbf{q}}, \mathcal{K}_{hc}). \quad (2)$$

The expressions  $\mathcal{K}_{ho}$ ,  $\mathcal{K}_{hc}$  contain the stiffness matrix of the spatial spring and the coupling spring parameters, respectively. The potential for the coupling springs is different from the potentials for spatial springs and is chosen to be spherical for each fingertip  $i$  [9]:

$$V_{hc}(\bar{\mathbf{q}}, \mathcal{K}_{hc}) = \frac{1}{2} \sum_{i=1}^N K_{hc,i} [\|\Delta \mathbf{p}_i(\bar{\mathbf{q}}) - \mathbf{l}_{i,d}\|]^2, \quad (3)$$

with  $\Delta \mathbf{p}_i(\bar{\mathbf{q}}) = \mathbf{p}_i(\bar{\mathbf{q}}) - \mathbf{p}_{ho}(\bar{\mathbf{q}})$  being the distance from the position of the fingertip frame  $i$  to the virtual object frame position  $\mathbf{p}_{ho}$ , and  $K_{hc,i} > 0$  the corresponding coupling stiffness.

### B. Employing Impedance Control for Two-Handed Manipulation

A natural extension of the impedance control approaches for the arms and hands allows to formulate intuitive compliance behaviors also for more complex anthropomorphic manipulators like the upper body of the humanoid *Justin* (Fig. 1). This system was built at DLR as a testbed for studying two-handed manipulation tasks. It consists of two four-fingered artificial hands, two light-weight arms, and a sensor head mounted on a movable torso including the neck. Overall, Justin has 43 degrees of freedom.

In this case there are virtual object frames for the right and the left arm  $\mathbf{H}_{r,o}(\bar{\mathbf{q}})$  and  $\mathbf{H}_{l,o}(\bar{\mathbf{q}})$ . Similar to multifingered hands, the compliance control in between the two hands has to handle the interaction forces between the two arms as well as the forces which they exert cooperatively on the environment. The implementation, however, is even simpler in this case and can be done by combining two spatial springs. One spatial spring defines the relative compliance between the arms and can be described in a straight-forward way by the potential function  $V_s(\mathbf{H}_{r,o}(\bar{\mathbf{q}}), \mathbf{H}_{l,o}(\bar{\mathbf{q}}), \mathcal{K}_c)$ . For implementing the cooperative action of the two hands it is useful to rely on a virtual object frame  $\mathbf{H}_o(\mathbf{H}_{r,o}(\bar{\mathbf{q}}), \mathbf{H}_{l,o}(\bar{\mathbf{q}}))$  depending on the two virtual object frames. This object frame describes a relevant pose in between the hands (usually just the mean between the pose of the right and left hand frame) and thus represents the pose of a grasped object. This virtual object is then connected via a spatial spring

$\mathcal{K}_o$  to a virtual equilibrium pose  $\mathbf{H}_{o,d}$ . In combination with the coupling stiffness, one thus can intuitively define an impedance behavior which is useful for grasping large objects with two hands. This compliance behavior can easily be combined with the potentials related to internal forces (Fig. 7). The complete potential function is then given by

$$V_P(\bar{\mathbf{q}}) = V_s(\mathbf{H}_o(\mathbf{H}_{r,o}(\bar{\mathbf{q}}), \mathbf{H}_{l,o}(\bar{\mathbf{q}})), \mathbf{H}_{o,d}, \mathcal{K}_o) + V_s(\mathbf{H}_{r,o}(\bar{\mathbf{q}}), \mathbf{H}_{l,o}(\bar{\mathbf{q}}), \mathcal{K}_c) + V_{hcr}(\bar{\mathbf{q}}, \mathcal{K}_{hcr}) + V_{hcl}(\bar{\mathbf{q}}, \mathcal{K}_{hcl}) . \quad (4)$$

Notice that all spatial springs generate joint torques for the arms, hands, as well as for the torso by computing the total derivative of the potential function with respect to the generalized coordinates of the complete mechanism (c.f. (1)). The presented control approach results in a passive closed loop system by design, and it is therefore related to other intuitive passivity based control approaches like the IPC [10]. Moreover, the chosen set of virtual spatial springs allows for a conceptually simple physical interpretation and consequently for an intuitive parametrization in any higher-level planning stage. An important feature is the realization of object forces and internal forces implicitly with impedances. In case of position uncertainties, that could be due to errors in modeling or localization, the object robot system will reach a stable equilibrium.

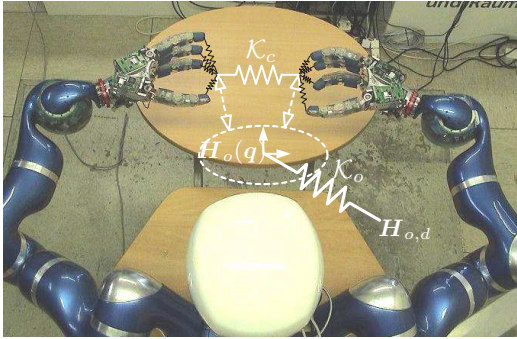


Fig. 7. Two-hand impedance behavior by combining the object level impedances of the hands and the arms.

#### IV. ROBOTIC HAND DESIGN TO COPE WITH UNCERTAINTY INTRINSICALLY

Human joints are actuated antagonistically. Every degree of freedom (DoF) has an agonist and an antagonist muscle. This is inevitable since human muscles are only able to produce tensile force. Since the muscles, tendons and ligaments are compliant having nonlinear stiffness characteristics, the human is able to adjust the joint stiffness a priori by activating agonist and antagonist simultaneously. Therefore, especially in known or predictable situations, the human is able to adapt his stiffness to prepare for impact.

In humans, the elasticity provided by the muscles, tendons and ligaments decouples the link position from the drive position by storing energy. Generally speaking, the energy introduced into the system, no matter whether caused by a

collision, external forces or acceleration of the link inertia is converted to elastic energy. This power source can be used to regain kinetic energy and therefore enhance the dynamics of the system, e.g. flipping small objects.

To improve positioning accuracy most robots are currently built as stiff as possible. Compliance of these *stiff robots* is, in most cases, realized using impedance control as presented in the previous section. Impedance control enables an "active", respectively controlled, compliance by means of a feedback controller running at a specific sampling rate. To reach the desired compliance the inertia of the robot and in particular the drives need to be accelerated to desired position and speed. Haddadin [11] has shown that the peak load during impact of the impedance controlled DLR LBR III occurs too fast to be measured in time by the joint torque sensors. Consequently, any *stiff robot* using "active compliance" appears stiff in case of collision.

In [12], Wolf shows that the actuation systems used within the DLR Hand Arm System can produce a link speed 2.6 times the drive speed using the energy stored in the elastic elements. In case of collision the decoupling of drive and link, through to energy storage, results in lower peak torques on the drives. *Stiff robots* can not store energy. Therefore, any externally introduced energy has to be dissipated actively by the drives.

Still, it needs to be mentioned that this architecture requires twice the amount of drives to actuate the joints. Furthermore, modular hands can be attached to various robot arms since they are self-contained. The relocation of the drives in the forearm requires the use of a suitable arm.

In the following section a novel anthropomorphic robot hand with variable stiffness actuation is presented that is of human size, and possesses dynamics and force capabilities as well as grasping abilities close to the human archetype. First experimental results confirm our design concept.

Another contribution of this design is the consequent design methodology to derive anthropomorphic robots from biology: Since the spread between biological and technical systems is very large, the key to a robust and highly dynamic hand arm system is to understand the human in a functional way rather than seamlessly trying to copy it. At the same time "drawbacks" of the biological system are not transferred to the technical system while providing maximal performance [13]–[15].

In this section first the design consideration of the forearm, the wrist, and the hand are presented. An overview of the coordinated hand wrist control is given.

##### A. Forearm

The fingers are actuated via the ServoModules. A multi-turn winder transfers the rotational gear motion to the tendons. The compliance mechanism is similar to the one described in [13]. One difference is that the winder also acts as the first pulley of the "tan  $\alpha$  mechanism" (Fig. 8). This reduces the number of required pulleys.

The requirements for the actuators of the wrist and the forearm rotation are almost identical. Therefore, the compact

ServoModules were used in slightly modified versions. The required torques for the forearm rotation and wrist actuation are higher than the ones for finger actuation leading to a actuation using rods instead of tendons. This enables the use of the recently developed BAVS actuation [2].

### B. Wrist

The desired motion range of the wrist and the expected tendon forces demand a special wrist design (Fig. 9). A roller guidance, which minimizes the tendon elongation during the wrist motion was developed. It keeps friction small and undesired centering forces from the hand tendons low. The wrist is based on the principle of an antiparallelogram (Fig. 9). Crossing bars held at base and end allow for a pivoting motion without changing their respective length. This principle was extended to a spherical antiparallelogram mechanism, which allows for  $\pm 30^\circ$  sideways motion, as well as  $\pm 90^\circ$  flexion/extension of the wrist. It is designed to withstand 6.5 kN, i.e. the sum of the maximum tendon forces. The wrist is actuated by 4 ServoModules to allow for motion and partial stiffness adjustability.

### C. Hand

The hand is the most exposed part of the robot, although it has the smallest force capabilities. The required features are large dexterity, manipulation capabilities, and robustness against unwanted collisions. As the human hand is highly underactuated and uses several muscle/tendon synergies [16], which are not technically realizable, a plain copy of the human hand is not reasonable. The hand design has to be based on an abstraction of the fundamental functionalities of the human hand. To reduce the number of drives, DoFs which have relatively low impact on grasping abilities should be omitted. These missing DoFs have to be compensated functionally by the kinematics design of the hand [15].

Overall, the kinematics of the new hand (Fig. 9) is closely adapted to the human hand on a functional basis [15]. It consists of 19 independent DoFs<sup>4</sup> in order to reduce the number of necessary drives. The 2nd (PIP) and 3rd (DIP) finger joint of the ring and fifth finger are coupled to reduce the number of necessary actuators. The 5th DoF of the human thumb turned out to be of low relevance [15], [17] and has been omitted. To ensure proper opposition of the thumb and the 5th finger, an antagonistically driven 4 bar

<sup>4</sup>Thumb 4 DoF, index finger 4 DoFs, middle finger 4 DoFs, ringfinger 3 DoFs, 5th finger 4 DoFs

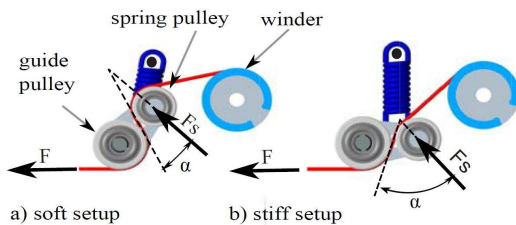


Fig. 8. Antagonistic drive compliance mechanism ("tan  $\alpha$  mechanism"): The pulley located at the spring loaded lever rotates around the center of the guiding pulley. Due to this design, a non-linear relation between tendon force and spring elongation is obtained. a) low mechanical stiffness due to small  $\alpha$  b) large  $\alpha$  results in high stiffness.

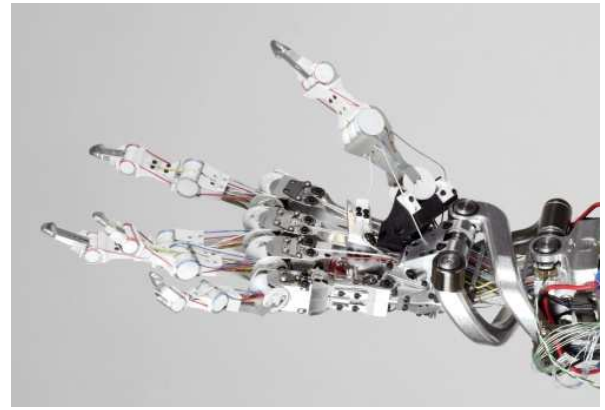


Fig. 9. Hand and wrist of the DLR Hand Arm System. Due to spacial restrictions, several sliding surfaces are used for the tendon routing. In order to ensure proper motion of the fingers even at high pretension, the palm design has to introduce minimal additional friction. Therefore, a palm design using ball bearing pulleys was realized.

mechanism was designed to mimic the motion of the 5th finger metacarpal bone<sup>5</sup>.

The structure of the finger is designed as an endoskeleton with *bionic joints* [14]. The finger base (metacarpal) joint is a hyperboloidally shaped saddle joint because the human condyloid joint type can not be replicated in a meaningful technical way. The finger (interphalangeal) joints, on the other hand, are designed as hinge joints. All joints allow dislocation without damage in case of overload<sup>6</sup>. In addition to robustness due to short-term energy storage, the use of antagonistic actuation enables to cope with tendon slackening or overstretching, which is one of the major problems of nowadays tendon-driven hands having inevitably constant tendon length. In contrast, antagonistic actuation is able to compensate unaligned pulley axes, and other geometrical errors via the elastic elements of the drive train. Therefore, no explicit tendon tensioner is needed [13].

### D. Wrist/Hand Control

The major task of the wrist/hand control is to deal with the large number of actuators and its kinematic joint couplings.

A controller was designed that accepts the joint position and mechanical joint stiffness as input values using the properties of the antagonistic motor/tendon arrangement. However, the tendon routing does not allow for an arbitrary intrinsic stiffness matrix. To increase the compliance range an impedance controller is used in series with the progressive springs. The control scheme implemented on the system for the finger/wrist control is depicted in Fig. 10. It assumes that the singular perturbation hypothesis is holding. Therefore, the joint control and the tendon control are analyzed independently. The inputs of the impedance block are the reference joint trajectories and the current joint positions. According to the user defined impedance, it leads to the desired joint torques that can be mapped to the tendon forces

<sup>5</sup>the first bone of the finger located within the palm

<sup>6</sup>the elongation of the tendons in case of dislocation is compensated by the elastic elements of the antagonistic drives

(Fig. 10, B) by using the kinematic structure. The tendon forces are finally given as references to the underlying tendon force controller (Fig. 10, C). A kinematic model of the wrist is used to compensate for the tendon displacement due to motion of the wrist (Fig. 10, A). The controller must ensure a constant pulling constraint to avoid slack, and needs to prevent excessive force on the tendons (Fig. 10, D). Hence, the safety block D provides a boundary limitation, for minimum and maximum tendon forces, via a saturation of the reference forces.

This controller represents a starting point from which a coordinated control architecture can be developed in order to fully exploit the system performances. For a more detailed description of similar controllers refer to [18].

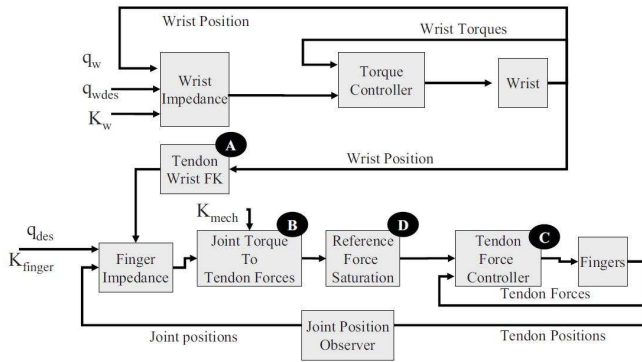


Fig. 10. Hand controller structure, the blocks marked with a letter are described in more details in the text (FK stands for forward kinematics).

## V. PRELIMINARY EXPERIMENTS WITH THE VARIABLE STIFFNESS HAND

Impact tests have been performed to verify the robustness of the DLR Hand Arm System. E.g. the fingers of the hand have been hit with a 500 g hammer, while being in position control without any damage. As a first simple demonstration of the full system robustness a nail has been driven into wood (Fig. 11). The trajectory was taught and uses no sensory feedback.



Fig. 11. Sequence of the DLR Hand Arm System driving a nail into solid wood using a 500 g standard hammer.

## VI. CONCLUSIONS

In this paper we gave an overview on the DLR activities related to two approaches for compliant dexterous manipulation tasks: actively torque controlled light-weight robots and variable stiffness actuated systems. Both robot prototypes are tolerant to uncertainty in position measurements. Since no controller switching in the contact transition is needed, the

concepts are also tolerant versus uncertainties in detecting collision.

Based on our experience with torque controlled robotic hands, we presented a critical analysis on the advantages and also disadvantages of VS driven hands. Furthermore, the design of the hand of the DLR hand arm system, which is motivated by this analysis, was presented.

## REFERENCES

- [1] A. Albu-Schäffer, O. Eiberger, M. Grebenstein, S. Haddadin, C. Ott, T. Wimböck, S. Wolf, and G. Hirzinger, "Soft robotics," *Robotics Automation Magazine, IEEE*, vol. 15, no. 3, pp. 20–30, sep. 2008.
- [2] M. Grebenstein, A. Albu-Schäffer, T. Bahls, M. Chalon, O. Eiberger, W. Friedl, R. Gruber, S. Haddadin, U. Hagn, R. Haslinger, H. Höppner, S. Jrg, M. Nickl, A. Nothhelfer, F. Petit, J. Reill, N. Seitz, T. Wimböck, S. Wolf, T. Wüsthoff, and G. Hirzinger, "The dlr hand arm system," in *accepted for the 2011 IEEE International Conference on Robotics and Automation, Shanghai/China*, 2011.
- [3] A. Albu-Schäffer, Ch. Ott, and G. Hirzinger, "A unified passivity based control framework for position, torque and impedance control of flexible joint robots," *International Journal of Robotics Research*, vol. 26, no. 1, pp. 23–39, January 2007.
- [4] Ch. Ott, A. Albu-Schäffer, A. Kugi, and G. Hirzinger, "On the passivity based impedance control of flexible joint robots," *IEEE Transactions on Robotics*, vol. 24, no. 2, pp. 416–429, April 2008.
- [5] A. Albu-Schäffer, Ch. Ott, and G. Hirzinger, "A passivity based cartesian impedance controller for flexible joint robots - part II: Full state feedback, impedance design and experiments," in *IEEE International Conference on Robotics and Automation*, 2004, pp. 2666–2672.
- [6] E. Fasse and J. Broenink, "A spatial impedance controller for robotic manipulation," *IEEE Transactions on Robotics and Automation*, vol. 13, no. 4, pp. 546–556, 1997.
- [7] F. Caccavale, C. Natale, B. Siciliano, and L. Villani, "Six-dof impedance control based on angle/axis representations," *IEEE Transactions on Robotics and Automation*, vol. 15, no. 2, pp. 289–299, 1999.
- [8] S. Stramigioli and V. Duindam, "Variable spatial springs for robot control applications," in *IEEE/RSJ International Conference on Intelligent Robots and Systems*, 2001, pp. 1906–1911.
- [9] T. Wimböck, Ch. Ott, and G. Hirzinger, "Passivity-based object-level impedance control for a multifingered hand," in *IEEE/RSJ International Conference on Intelligent Robots and Systems*, 2006, pp. 4621–4627.
- [10] S. Stramigioli, *Modeling and IPC Control of Interactive Mechanical Systems: A Coordinate-free Approach*, ser. Lecture Notes in Control and Information Sciences. Springer-Verlag, 2001, vol. 266.
- [11] S. Haddadin, A. Albu-Schäffer, O. Eiberger, and G. Hirzinger, "New insights concerning intrinsic joint elasticity for safety," in *Proc. IEEE/RSJ International Conf. on Intelligent Robots and Systems (IROS)*, Taipei, Taiwan, 2010, pp. 2181–2187.
- [12] S. Wolf and G. Hirzinger, "A new variable stiffness design: Matching requirements of the next robot generation," in *Proc. IEEE International Conf. on Robotics and Automation (ICRA)*, 2008, p. 1741–1746.
- [13] M. Grebenstein and P. van der Smagt, "Antagonism for a highly anthropomorphic HandArmSystem," *Advanced Robotics*, no. 22, pp. 39–55, 2008.
- [14] M. Grebenstein, M. Chalon, G. Hirzinger, and R. Siegart, "Antagonistically driven finger design for the anthropomorphic DLR hand arm system," in *Proc. IEEE-RAS International Conference on Humanoid Robots (HUMANOIDS)*, 2010.
- [15] —, "A method for hand kinematics designers; 7 billion perfect hands," in *Proc. International Conference on Applied Bionics and Biomechanics (ICABB)*, 2010.
- [16] H. Gray, *Anatomy, descriptive and surgical*. Philadelphia: Courage Books, 1999.
- [17] M. Chalon, M. Grebenstein, T. Wimboeck, and G. Hirzinger, "The thumb: Guidelines for a robotic design," in *Proc. IEEE/RSJ International Conf. on Intelligent Robots and Systems (IROS)*, 2010.
- [18] T. Wimböck, Ch. Ott, A. Albu-Schäffer, A. Kugi, and G. Hirzinger, "Impedance control for variable stiffness mechanisms with nonlinear joint coupling," in *IEEE/RSJ International Conference on Intelligent Robots and Systems*, 2008, pp. 3796–3803.